Acta Cryst. (1997). B**53**, 928–938

Rigid-Body Disorder Models for the High-Temperature Phase of Ferrocene

CAROLYN PRATT BROCK* AND YIGANG FU

Department of Chemistry, University of Kentucky, Lexington, KY 40506-0055, USA. E-mail: cpbrock@ukcc.uky.edu

(*Received 12 June 1996; accepted 3 April 1997*)

Abstract

Ferrocene, $[Fe(C_5H_5)_2]$, which crystallizes at room temperature in space group $P2_1/a$ with $Z = 2$, is described in many textbooks as having D_{5d} symmetry. Previous work has shown, however, that the librational amplitude associated with motion about the fivefold axis does not decrease with temperature and that the crystals are probably disordered. Ferrocene molecules in triclinic crystals grown below 169 K have approximate D_5 symmetry and an almost eclipsed conformation; the low- and high-temperature phases may be related by an order–disorder transition, during which the number of independent atoms changes by a factor of 4. The structure of the high-temperature phase has been reinvestigated with rigid-body refinements of the neutron diffraction data collected at 173 and 298 K by Takusagawa & Koetzle [*Acta Cryst.* (1979), B**35**, 1074–1081]. The C_5H_5 ring was treated as a rigid group of C_5 symmetry; C—C and C—H distances were allowed to vary, as was the displacement of the H atoms from the C_5 plane. The rigid-body motion of the C_5H_5 ligand was described by the **TLS** model. All the rigid-body disorder models fit better than conventional independent-atom models. A disorder model that includes three sites for each C_5H_5 ring is the best of the models that were investigated, which indicates that the structure of the high-temperature phase cannot be described by the superposition of the two independent ferrocene molecules in the low-temperature phase. The phase transition between the high- and low-temperature phases is not a simple order–disorder transition.

1. Introduction

Ferrocene {bis(cyclopentadienyl)iron, $[Fe(C_5H_5)_2]$} crystallizes in the monoclinic space group $P2_1/a$ with two molecules per unit cell (Fischer & Pfab, 1952; Eiland & Pepinsky, 1952; Dunitz & Orgel, 1953). The Fe atoms are located on inversion centers and the molecule must, at least on average, conform to $\bar{1}$ point symmetry. A more detailed three-dimensional structure analysis by Dunitz, Orgel & Rich (1956; hereafter DOR) confirmed approximate D_{5d} symmetry, but showed smearing of the electron-density maxima in the plane of the cyclopentadienyl ring.

Heat capacity measurements in the ranges 125–200 K (Edwards, Kington & Mason, 1960) and 17–300 K (Edwards & Kington, 1962) revealed a λ-point transition ($\Delta H = 0.854$ kJ mol^{-1}; $\Delta S = 5.29$ J K^{-1} mol^{-1} = Rln 1.89) at 163.9 K with a secondary Cp maximum at 169 K. The λ-point transition was interpreted in terms of rotational disorder of the cyclopentadienyl rings. Rotational disorder in the monoclinic high-temperature phase of ferrocene was demonstrated by Willis (1960, 1961), who measured neutron diffraction data. Willis proposed a random mixture of staggered molecules in two orientations: DOR and anti-DOR (rotated by 36°) orientations. The best agreement factor corresponded to a 2:1 ratio of the ring position found by DOR and the position generated by a 36° rotation around the approximate fivefold axis.

Years later the structure of the high-temperature phase was studied again by Seiler & Dunitz (1979*a*; hereafter SD) and Takusagawa & Koetzle (1979; hereafter TK). SD found the mean-square librational amplitude about the axis perpendicular to the cyclopentadienyl (hereafter, Cp) ring to be both very large [r.m.s. angular displacement (*ca* 15°) 20% of the displacement (*ca* 72°) between C-atom sites] and to be almost independent of temperature [231 (27) deg^2 at 173 K and 220 (30) deg^2 at 293 K]. This behavior was taken as evidence of disorder. Refinement of an isotropic twofold split-atom disorder model suggested that the ring centers for the two sites were slightly offset.

TK used neutron diffraction data measured at 298 and 173 K to refine three models: (*a*) a conventional anisotropic model; (*b*) a model including anharmonic displacement parameters; (*c*) a twofold disorder model with anisotropic displacement parameters (hereafter, ADP's). The first model gave results similar to those found by SD. The second model gave the best fit, which suggested that the disorder might involve a continuous range of molecular configurations. The ratio of observations to variable parameters for the anharmonic model was, however, very small (see Table 1). The third model, which converged poorly, gave results qualitatively the same as those for SD's disorder model. The neutron study also revealed that the H atoms of the Cp rings are displaced toward the Fe atom by an average of 0.030 Å.

The high-temperature phase of ferrocene was also studied by Calvarin, Berar & Clec'h (1982). The X-ray data they measured to 0.71 Å^{-1} at 295 K were refined with a rigid-body model having D_5 symmetry, fixed bond lengths and angles, and two variable B values (one for the

Table 1. *Summary of refinements*

Model	NV	*R*, *wR* (173 K)	*R*, *wR* (298 K)
TK (*A*)	99	0.121, 0.122	0.130, 0.082
		(0.124, 0.122)†	**(0.075, 0.079)†**
TK (*B*)	349	0.053, 0.053	0.049, 0.032
TK (*C*)	189	0.072, 0.071	0.060, 0.044
R1	33	0.157, 0.164	0.104, 0.118
R1Z	36	0.144, 0.151	0.104, 0.118
R1ZH	37	0.144, 0.150	0.102, 0.115
R2	59	0.083, 0.080	0.046, 0.046
R2Z	62	0.074, 0.071	0.042, 0.043
R2ZH	64	0.071, 0.068	0.040, 0.041
R2ZHO	65	0.069, 0.066	0.037, 0.036
R4ZHO	58	0.066, 0.063	0.035, 0.036
R3ZHO	93	0.061, 0.059	0.031, 0.031

† As repeated in this work. N_{obs} = 776 (of 930 intensities measured) at 173 K and 369 (of 687 intensities measured) at 298 K.

Fe atom, the other for the C and H atoms). Models with one, two, three and four independent molecules (two, four, six and eight independent rings) were tried. The four-ring model (two independent molecules with variable internal rotations; neither molecule fixed at the origin; *ca* 20 variables) gave the best fit (R = 0.060, wR = 0.061). The ratio of the occupancy factors was set at 2:1, although the quality of the fit for a 1:1 ratio was similar. Energy calculations also suggested a four-ring model, in this case with occupancy factors ranging from 0.20 to 0.29.

The structure of the low-temperature phase of ferrocene has also been studied extensively (Calvarin & Berar, 1975; Clec'h, Calvarin, Berar & Kahn, 1978; Seiler & Dunitz, 1979*b*; Calvarin, Clec'h, Berar & André, 1982). Seiler & Dunitz (1979*b*) grew a single crystal below 160 K to avoid the twinning that results from cooling through the transition. The two independent molecules in the triclinic low-temperature phase have approximate D_5 symmetry, but are neither eclipsed nor staggered; the rings within each molecule are offset by *ca* 9°. SD then suggested that the formally centrosymmetric ferrocene molecule of the disordered monoclinic high-temperature phase of ferrocene might be described as an averaged superposition of the two independent ferrocene molecules of the triclinic low-temperature cell.

The many studies of ferrocene have been reviewed by Braga (1992) and by Dunitz (1993, 1995).

Although the high-temperature phase of ferrocene has been studied extensively, none of the models provides a physically reasonable description of the thermal motion. We hoped that the use of a model incorporating the TLS model for rigid-body motion (Schomaker & Trueblood, 1968) might lead to a more satisfactory description.

2. Methodology

2.1. *Data*

Takusagawa & Koetzle's (1979) neutron diffraction data were used in this study because the H-atom contributions to the scattering break the conic section singularity (Cruickshank, 1956; Schomaker & Trueblood, 1968) associated with a C_5 ring. Data provided by Koetzle had already been corrected for absorption and extinction. Structure factors for 930 independent reflections measured at 173 K [$(\sin\theta/\lambda)_{max} < 0.68$; $(F/\sigma_F)_{min} = 2.6$; $\langle F/\sigma_F\rangle = 24.3$] and 687 measured at 298 K [$(\sin\theta/\lambda)_{max} < 0.62$; $(F/\sigma_F)_{min} = 0.1$; $\langle F/\sigma_F\rangle = 12.5$] were available. The 00$l$ and 20l reflections were missing from the 298 K data and seem to have been lost.

The neutron scattering lengths (all $\times 10^{-11}$ mm) are b_C = 0.665, b_H = −0.374 (Koester & Yelon, 1983); the starting value for b_{Fe} was 0.924 at 298 K and 0.902 at 173 K (Takusagawa & Koetzle, 1979). Koester & Yelon (1983) give a different value for b_{Fe} (0.954), but variation of the neutron scattering length has little effect on the refinement.

Cell constants determined by TK are a = 10.443 (5), b = 7.572 (4), c = 5.824 (4) Å, β = 120.95 (8)° at 173 K, and a = 10.530 (8), b = 7.604 (5), c = 5.921 (4)Å, β = 121.05 (8)° at 298 K.

2.2. *Programs*

Least-squares refinements were performed with a highly modified version of the program *ORFLS* (Busing, Martin & Levy, 1962). The TLS rigid-body refinements used Shmueli & Goldberg's (1974) subroutines (see Brock, Blackburn & Haller, 1984) and Strouse's (1970) method for varying rigid-body distances and angles. The function minimized was $\Sigma w(|F_o| - |F_c|)^2$, where $|F_o|$ and $|F_c|$ are the observed and calculated structure-factor amplitudes and the weight w is $4F_o^2/[\sigma^2(F_o^2)]$.

TK's independent-atom model (*A*) was refined as a check. The 98 variables included the coherent neutron scattering length of the Fe atom and a scale factor. (The data provided by TK had already been corrected for extinction.) TK used all reflections with $F_o^2 < 3\sigma(F_o^2)$ in their refinements, but did not give N_{obs}. We found that this criterion was met by 776 of the 930 structure factors measured at 173 K and by 369 of the 687 measured at 298 K.

The coordinates and ADP's from our refinement agree well with TK's results at both temperatures, but our e.s.d.'s are almost twice as large as theirs. For the 173 K data the agreement factors (R = 0.124; wR = 0.122) are quite close to TK's values (0.121; 0.122), but for the 298 K data our agreement factors (0.075; 0.079) are significantly lower than theirs (0.130; 0.082). Attempts to reconcile this inconsistency were unsuccessful.

2.3. *Rigid-body geometry*

The Cp ring was assumed to have C_{5v} symmetry. The origin of the Cartesian system is at the center of the C_5 ring, the x axis points toward C(4) and the z axis is perpendicular to the C_5 ring. Starting geometries were

Table 2. *Ratios* $T^{ii}_{298}/T^{ii}_{173}$ *and* $L^{ii}_{298}/L^{ii}_{173}$ *(298/173 = 1.72)*

Model	NV	$T^{ii}_{298}/T^{ii}_{173}$			$L^{ii}_{298}/L^{ii}_{173}$		
R1	33	1.6 (1)	1.5 (1)	2.2 (6)	1.2 (2)	1.2 (2)	1.06 (5)
R1Z	36	1.7 (1)	1.6 (1)	2.0 (5)	1.2 (2)	1.3 (2)	1.09 (5)
R1ZH	37	1.6 (1)	1.6 (1)	1.5 (2)	1.3 (5)	1.5 (5)	0.97 (6)
R2	59	2.0 (2)	2.1 (2)	2.5 (9)	1.2 (2)	1.3 (2)	1.8 (2)
		1.4 (1)	1.8 (1)	1.8 (6)	1.3 (2)	1.4 (3)	1.2 (1)
R2Z	62	1.8 (2)	2.0 (2)	1.9 (6)	1.4 (2)	1.6 (2)	1.4 (1)
		1.4 (1)	1.6 (1)	1.8 (6)	1.2 (2)	1.3 (2)	0.9 (1)
R2ZH	64	1.7 (1)	2.0 (1)	1.5 (2)	2.0 (7)	2.3 (10)	1.1 (2)
		1.4 (1)	1.6 (1)	1.3 (2)	1.4 (5)	1.8 (6)	1.0 (1)
R2ZHO	65	1.4 (1)	1.8 (1)	1.4 (2)	2.1 (5)	2.1 (6)	1.0 (1)
		1.6 (2)	1.7 (2)	1.5 (3)	1.0 (5)	1.6 (7)	1.3 (2)
R4ZHO	58	1.7 (1)	1.6 (1)	1.5 (2)	1.9 (3)	1.8 (3)	1.2 (4)
R3ZHO	93	1.7 (3)	1.6 (1)	1.4 (4)	2.1 (10)	2.7 (11)	2.3 (8)
		1.3 (1)	2.2 (3)	1.9 (5)	2.1 (6)	1.1 (5)	0.9 (3)
		1.9 (3)	1.1 (2)	1.1 (3)	0.5 (6)	3.9 (22)	2.1 (7)

taken from TK's unconstrained refinement model (*c*) (Takusagawa & Koetzle, 1979): *r*(C—C) = 1.418 and *r*(C—H) = 1.042 Å at 173 K; *r*(C—C) = 1.398 and *r*(C—H) = 1.022 Å at 298 K; H atoms displaced away from the C_5 ring and towards the Fe atom by $\Delta_H = 0.030$ Å. The apparent decrease in the bond lengths with increased temperature reflects the greater thermal motion. Three totally symmetric distortions were allowed: radial displacements of the C atoms, radial displacements of the H atoms and H-atom displacements perpendicular to the C-atom plane.

We considered including the Fe atom in the rigid body, but chose not to do so because doing so would require that displacements associated with certain internal modes be zero. Setting the origin of the C_5H_5 group at the origin also introduces constraints. The molecule was described as nonrigid by Seiler & Dunitz (1979*b*, 1980), who pointed to evidence for the vibration of the C_5 framework relative to the Fe atom. Seiler & Dunitz (1979, 1980) included the Fe atom in their TL(S) analyses, but apparently did so only to break the conic section singularity.

2.4. *Variables*

Six variables (three coordinates and three orientations) specify the positions of the rigid Cp ring. Three additional variables (see above) allow optimization of the Cp geometry. The TLS model requires 20 parameters for each rigid body: six each for the symmetric *T* and *L* tensors, and eight for the *S* tensor. (The trace of *S*, which is indeterminate, was set to zero.) The Fe-atom coordinates are fixed by symmetry; its anisotropic displacement ellipsoid requires six parameters. All refinements converged $[(\Delta/\sigma)_{max} < 0.15]$ without problems, except as discussed below.

2.5. *H-atom motion*

Although the C_5 ring is expected to be effectively rigid, the internal (or excess) motion of the H atoms can be assumed to be important. Johnson (1970) calculated the mean-square displacements of the H atoms in gaseous benzene as 0.005 (bond stretch), 0.013 (in-plane tangential) and 0.021 Å^2 (out-of-plane). Corrections for the latter two motions were included under the assumption that the total vibrational amplitude of the H atom is the algebraic sum of the rigid-body motion and the internal motion ($\mathbf{U}_H = \mathbf{U}_R + \mathbf{U}_{int}$).

The internal in-plane tangential motion of the H atoms was described by an extra L^{33} term and the out-of-plane internal motion by an extra T^{33} term. The extra T^{33} term was fixed at the value (0.021 Å^2) determined for benzene (Johnson, 1970).

2.6. *Criteria*

Two criteria were used to judge the refinement results of the different structural models. The first was Hamilton's *R*-value test (Hamilton, 1965; Pawley, 1970). The value of the test parameter was calculated according to the approximate method developed by Pawley (1970). The confidence level required was 99%.

The second criterion was the temperature dependence of the displacement parameters. Maverick & Dunitz (1987) showed that the temperature dependence of the displacement parameters for a fivefold sinusoidal potential is about the same as for a quadratic potential. The mean-square amplitude should then be proportional to absolute temperature, at least as long as the potential-energy function is harmonic, the temperature is high and the vibrational amplitudes are relatively low. The temperature must be high enough that the effect of the zero-point motion on the shape of the curve is not important; this condition is usually met as long as $T > 100$ K. The vibrational amplitudes must be small enough that the quadratic approximation and the assumption of infinitesimal rotations introduce no significant errors. Trueblood (1978) claimed that these two conditions are met if the mean-square librational amplitude is below *ca* 500 deg^2.

Table 3. *Parameters for model R1ZH*

	At 173 K	At 298 K
x	0.1140 (3)	0.1138 (8)
y	0.1557 (3)	0.1548 (5)
z	0.0161 (6)	0.0206 (9)
φ (°)†	56.5 (1)	56.6 (2)
θ (°)	158.9 (2)	158.5 (3)
ρ (°)	−108.6 (1)	−108.3 (2)
r(C—C) (Å)	1.388 (2)	1.396 (6)
r(C—H) (Å)	1.076 (6)	1.010 (11)
Δ_H (Å)	0.029 (7)	0.016 (11)
$(\Delta/\sigma)_{max}$	0.14	0.10

† Angles φ, θ and ρ are those defined by Strouse (1970).

Additional details about the refinement procedures and results can be found in the Ph.D. thesis of Fu (1991)†.

3. Results

3.1. *One-ring models*

Models composed of a single Cp ring were included so that comparisons could be made with TK's independent-atom model (*A*) and so that the importance of varying the ring geometry and the H-atom motion could be determined. Initial coordinates of the two Cp rings were derived from TK's model (*A*). The initial values of the diagonal components of the **T** and **L** tensors at 173 K were derived by multiplying the values found at 148 K by Seiler & Dunitz (1979*b*) by the factor (173/148). The off-diagonal parameters of the **T**, **L** and **S** tensors, all initially zero, were varied only after preliminary convergence. Refinement of the 298 K data started from the parameters determined for the 173 K data. A scale factor, six anisotropic displacement parameters for the Fe atom, the three positional and three orientation parameters of the ring were varied. Three models were tried: (i) R1: No geometry optimization; no variation of H-atom internal motion. (ii) R1Z: Geometry of Cp ring optimized. (iii) R1ZH: Two L^{33} parameters, one for the five C atoms and one for the five H atoms, varied.

The agreement factors (Table 1) are somewhat higher than for TK's independent-atom model (*A*), but the number of variables is much reduced. The extra degrees of freedom in models R1Z and R1ZH are more important for the 173 K structure in which the atom distributions are more sharply defined than they are for the 298 K structure. During refinement the bond lengths at 298 K changed only slightly, but the C—H bond length at 173 K changed by −0.027 (2) Å (see Table 3). The atomic displacement ellipsoids (see Fig. 1) look very much like those shown by previous authors. The temperature dependence for most of the T^{ii} and L^{ii} values (see Tables 2 and 4) is reasonably normal, but the value of L^{33} is, as expected, approximately constant. A final difference map (Fig. 2) reveals important peaks and troughs.

The capacity of the TLS model to fit atoms C(2) and C(3), which are relatively 'compact', as well as atoms C(4) and C(5), which are much more 'extended', is noteworthy. Although the origin of the coordinate system for **L** is fixed at the center of the C_5 ring, the correlation (or screw) tensor **S** allows the tangential motion of the five C (and H) atoms to vary.

3.2. *Superposition results*

Seiler & Dunitz (1979*a*) chose a nonstandard space group ($F\bar{1}$; $Z = 16$; $Z' = 2$) for the low-temperature phase of ferrocene to highlight its similarity to the high-temperature phase ($P2_1/a$; $Z = 2$; $Z' = 1/2$). The axes of the low-temperature phase are nearly twice as long as the corresponding axes of the high-temperature phase and the three angles are similar. In the low-temperature phase

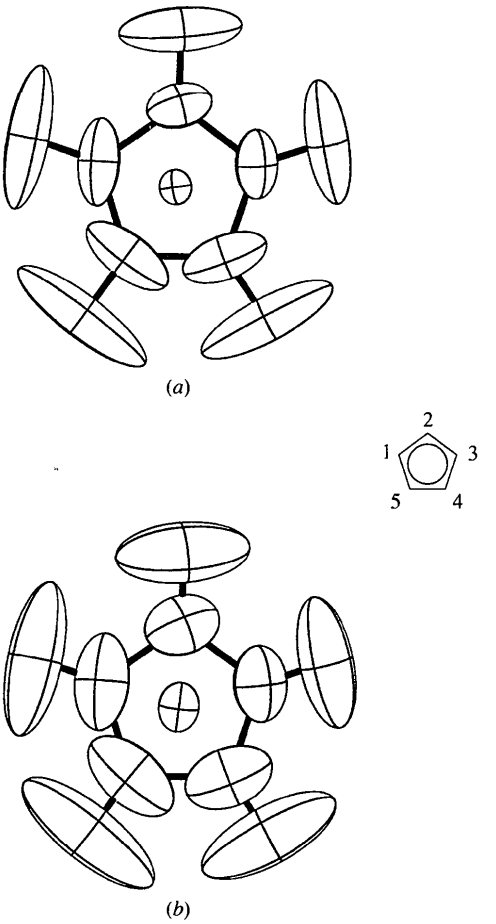

Fig. 1. Ellipsoid plots of the asymmetric unit after refinement with model R1ZH at (*a*) 173 and (*b*) 298 K. The ellipsoids here and in the remaining figures are drawn at the 50% probability level.

† Lists of atomic coordinates, positional parameters and neutron diffraction data have been deposited with the IUCr (Reference: CR0517). Copies may be obtained through The Managing Editor, International Union of Crystallography, 5 Abbey Square, Chester CH1 2HU, England.

Table 4. *Thermal motion description for the model R1ZH*

	At 173 K			At 298 K		
U_{Fe} (Å^2)	0.027 (2)	−0.005 (1)	0.016 (1)	0.040 (4)	−0.007 (3)	0.029 (4)
		0.020 (1)	−0.002 (1)		0.036 (3)	−0.005 (3)
			0.031 (2)			0.062 (4)
T (Å^2)	0.042 (2)	0.001 (1)	−0.002 (1)	0.069 (4)	−0.004 (2)	0.000(2)
		0.049 (2)	−0.005 (1)		0.081 (4)	−0.004 (2)
			0.021 (2)			0.031 (3)
L (deg^2)	18.0 (4)	2.0 (2)	4.0 (4)	24.0 (7)	5.0 (4)	−2.0 (7)
		18.0 (4)	−14.0 (4)		27.0 (7)	−12.0 (7)
			216.0 (6)			210.0 (11)
L_H^{33} (deg^2)			241.0 (10)			262.0 (14)
S (Å deg)	−0.20 (4)	0.26 (5)	−0.02 (3)	−0.27 (8)	0.50 (10)	0.02 (6)
	−0.31 (5)	−0.06 (4)	−0.09 (3)	−0.59 (9)	−0.05 (10)	−0.08 (5)
	−0.52 (6)	−1.33 (6)	0.26†	−0.24 (10)	−1.36 (12)	0.32†

† Determined by the constraint tr(**S**) = 0.

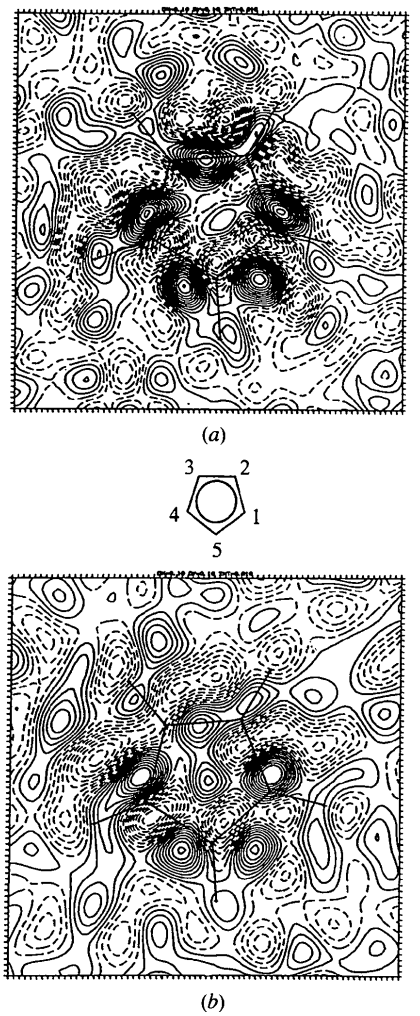

Fig. 2. Final difference maps through the best plane of the Cp ring calculated after refinement with model R1ZH at (*a*) 173 and (*b*) 298 K. Contours are at intervals of 0.016 mm Å^{-3} in (*a*) and 0.010 mm Å^{-3} in (*b*). Solid, broken and dashed lines denote positive, zero and negative contours. Since the scattering length of the H atom is negative, the H atoms in Fourier maps are associated with troughs rather than with peaks.

Table 5. *Parameters for model R2ZHO*

	At 173 K	At 298 K
x	0.1086 (5)	0.1086 (7)
	0.1232 (6)	0.1222 (9)
y	0.1598 (6)	0.1565 (6)
	0.1527 (8)	0.1563 (11)
z	0.0102 (7)	0.0095 (10)
	0.0398(14)	0.0502 (22)
φ (°)†	58.9 (2)	58.8 (3)
	51.1 (4)	49.9 (5)
θ (°)	153.1 (3)	154.1 (4)
	174.4 (6)	178.0 (22)
ρ (°)	−110.0 (2)	−109.9 (4)
	−105.8 (3)	−105.0 (5)
r(C—C) (Å)	1.405 (1)	1.403 (2)
r(C—H) (Å)	1.064 (3)	1.042 (5)
ΔH (Å)	0.032 (3)	0.031 (4)
Occupancy factors	0.61 (2)	0.64 (3)
	0.39	0.36
$(\Delta/\sigma)_{max}$	0.05	0.06

† Angles φ, θ and ρ are those defined by Strouse (1970).

there are four independent Cp rings, while in the high-temperature phase there is only one independent Cp ring.

Authors of previous studies have suggested that the high-temperature phase of ferrocene might be an averaged superposition of the molecules of the low-temperature cell with the long-range order of the low-temperature phase being lost during the transition at 164 K (Takusagawa & Koetzle, 1979; Seiler & Dunitz, 1979*a*). If this description is correct, the averaged superposition of the two independent molecules of the low-temperature phase must be close to the atomic distribution observed for the high-temperature phase. In order to examine the similarity of the structures, the low-temperature structure was projected onto the high-temperature cell.

The result of this superposition is shown in Fig. 3. The four Cp rings are all on the same 'side' of the Fe atom; another set of rings, related to the first by an inversion center, are on the other side of the Fe atom. The four rings are grouped into two sets of two; within each set of

two the atoms are very close together. Each of the two independent molecules contributes one ring to each set. Even though the individual ferrocene molecules of the low-temperature phase are not centrosymmetric, their superposition is well represented by a single centrosymmetric molecule.

3.3. *Two ring models*

If the transition between the triclinic and monoclinic phases is a simple order–disorder transition, the superposition model should be a good description of the high-temperature phase. The occupancy factor was 0.5 unless varied. Four models were tried: (i) R2: No geometry optimization; no variation of H-atom internal motion. (ii) R2Z: Geometry of Cp ring optimized. (iii) R2ZH: Two L^{33} parameters, one each for the five C atoms and five H atoms, varied. (iv) R2ZHO: Occupancy factor also varied.

The agreement factors (see Table 1) are much lower than for the one-ring models. Model R2ZHO (see Fig. 4) is the best of the four and is also better than TK's split-atom disorder model (*C*), even though R2ZHO has many fewer variables. When the 173 K data are refined with this model there is only one correlation coefficient with an absolute value greater than 0.80 (−0.84 for the y coordinates of the two rings). When the 298 K data are refined, however, this correlation coefficient rises to −0.89 and the correlation between the two L^{33} values becomes significant (0.82). The difference-Fourier maps for model R2ZHO (Fig. 5) are much cleaner than those for model R1ZH (Fig. 2).

The two Cp rings are separated by a *ca* 20° rotation about the approximate fivefold axis (see Fig. 4). The ring centers do not coincide, but are separated by 0.170 (5) Å at 173 K and 0.21 (1) Å at 298 K. The occupancy factor for ring 1 is 0.61 (2) at 173 K and 0.64 (3) at 298 K (see Table 5). The deviation of the occupancy factor from 0.5 is a strong indication that the atomic distribution in the high-temperature phase is not an averaged superposition of the distribution found in the low-temperature phase.

The expected temperature dependence of the L^{33} component is found in the simplest two-ring model (R2), but is lost as the model is made more flexible. In the R2ZHO model the L^{33} value of ring 2 increases by a factor of 1.29 when the temperature increases by a factor of 1.72 (see Tables 2 and 6). The L^{33} value of ring 1, however, is almost constant. The L^{11} and L^{22} values (averaged over the two rings) increase by factors of 1.5 and 1.8. As judged by this criterion, the two-ring model is not satisfactory.

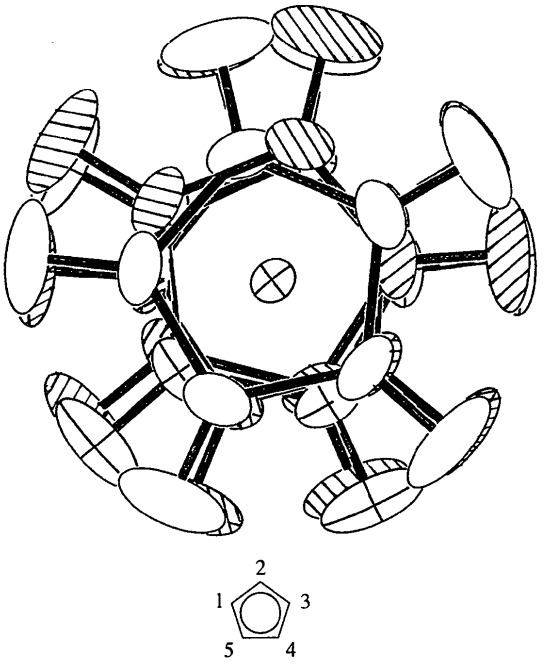

Fig. 3. Ellipsoid plots of a superposition (see text) of the two molecules of the low-temperature phase. Boundary ellipses only are drawn for molecule (I); both principal and boundary ellipses are drawn for molecule (II). One set of rings is hatched.

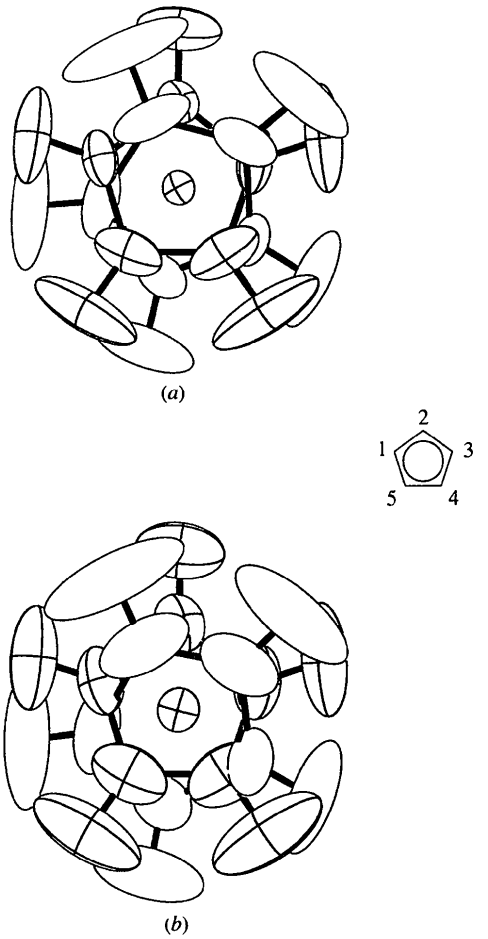

Fig. 4. Ellipsoid plots of the asymmetric unit after refinement with model R2ZHO at (*a*) 173 and (*b*) 298 K. The principal ellipses are drawn for ring 1 only.

Table 6. *Thermal motion description for the model R2ZHO*

	At 173 K			At 298 K		
$\mathbf{U}_{Fe}$ (Å^2)	0.0280 (8)	−0.0050 (6)	0.0159 (6)	0.0399 (13)	−0.0068 (10)	0.0244 (12)
		0.0200 (7)	−0.0018 (6)		0.0359 (10)	−0.0010 (12)
			0.0303 (8)			0.0518 (14)
T (Å^2)	0.044 (2)	−0.002 (1)	−0.005 (1)	0.064 (3)	−0.005 (1)	−0.003 (2)
	0.042 (4)	0.004 (2)	0.000 (2)	0.068 (6)	0.002 (3)	−0.003 (3)
		0.040 (2)	0.000 (1)		0.071 (3)	0.001 (2)
		0.031 (2)	−0.002 (1)		0.052 (4)	−0.002 (2)
			0.021 (2)			0.029 (3)
			0.023 (3)			0.035 (5)
L (deg^2)	17.0 (3)	1.0 (1)	10.0 (4)	35.0 (5)	0.0 (2)	7.0 (6)
	19.0 (5)	6.0 (3)	−17.0 (7)	19.0 (8)	5.0 (5)	−2.0 (11)
		14.0 (3)	10.0 (4)		29.0 (5)	0.0 (6)
		16.0 (5)	−12.0 (7)		25.0 (9)	−34.0 (13)
			101.0 (6)			102.0 (11)
			141.0 (12)			182.0 (23)
L_H^{33} (deg^2)			137.0 (6)			136.0 (9)
			182.0 (12)			225.0 (24)
S (Å deg)	−0.25 (4)	0.33 (5)	0.03 (3)	−0.17 (6)	0.55 (8)	0.06 (4)
	0.05 (8)	0.21 (6)	−0.02 (5)	0.25 (14)	0.46 (11)	0.00 (8)
	−0.39 (5)	−0.10 (4)	0.02 (3)	−0.52 (7)	−0.02 (6)	−0.04 (5)
	−0.26 (9)	0.06 (7)	−0.06 (5)	−0.72 (16)	0.31 (13)	0.08 (8)
	−1.09 (8)	−0.36 (6)	0.35†	−1.09 (11)	−0.43 (10)	0.20†
	1.07 (13)	0.52 (11)	−0.11†	1.30 (24)	0.93 (20)	−0.55†

† Determined by the constraint tr(**S**) = 0

3.4. *Four-ring models*

There are four independent cyclopentadienyl rings in the low-temperature phase of ferrocene. Four-ring models were tried because the two-ring models were unsatisfactory. Starting coordinates and orientation angles were calculated from the atomic coordinates of the low-temperature phase of ferrocene as measured at 148 K (Seiler & Dunitz, 1979*b*). The starting values of the TLS parameters were the same as for the one- and two-ring models. Occupancy factors were 0.25 initially.

The four-ring models were (as expected) plagued by large correlations. Even constrained refinements were unstable. All refinements, however, had a common feature: an initial superposition model (a 2 + 2 arrangement of the four rings; see Fig. 3) always converged to a 1 + 2 + 1 arrangement, in which the two central rings are nearly superimposed.

The most successful model, R4ZHO, allowed geometry optimization, separate L^{33} values for C and H atoms, and variation of occupancy factors; the four sets of TLS parameters, including the extra L^{33} value, were set equal. This model agrees with the data better than R2ZHO (see Table 1), even though R4ZHO has fewer variables. The improved agreement seems to be associated with the possibility of a more or less continuous, although peaked, distribution of scattering density about the approximate fivefold axis.

3.5. *Three-ring models*

Our experience with four-ring models suggested that three-ring models should be tried, even though such a model might not correspond to a simple disorder scheme.

Table 7. *Parameters for model R3ZHO*

	At 173 K	At 298 K
x	0.100 (2)	0.107 (2)
	0.119 (1)	0.111 (2)
	0.123 (1)	0.126 (1)
y	0.161 (2)	0.161 (2)
	0.156 (1)	0.153 (2)
	0.155 (1)	0.157 (2)
z	0.013 (2)	0.030 (3)
	0.015 (2)	0.002 (3)
	0.048 (2)	0.043 (3)
φ (°)†	63.1 (7)	61.7 (9)
	55.3 (4)	58.8 (6)
	48.4 (6)	49.3 (7)
θ (°)	146.5 (10)	144.3 (13)
	161.7 (6)	159.5 (6)
	180.5 (7)	176.3 (14)
ρ (°)	−112.2 (6)	−109.7 (7)
	−108.2 (4)	−110.2 (6)
	−105.3 (5)	−105.5 (8)
r(C—C) (Å)	1.415 (2)	1.406 (4)
r(C—H) (Å)	1.073 (3)	1.056 (6)
ΔH (Å)	0.031 (3)	0.030 (4)
Occupancy factors	0.31 (2)	0.37 (2)
	0.45 (2)	0.35 (2)
	0.24	0.28
$(\Delta/\sigma)_{max}$	0.04	0.03

† Angles φ, θ and ρ are those defined by Strouse (1980).

Only the most successful of the many three-ring models investigated will be discussed.

The positions and orientations of the two outer rings and one of the central rings in the model R4CZH were taken as the starting parameters. Starting values of the **TLS** parameters were the same as for the one-ring model.

Occupancy factors were initially 0.5 for the central ring and 0.25 for each of the outer rings.

Refinements were stable; different sets of starting parameters converged to the same set of final parameters (see Table 7). No damping (except of the deformation parameters) was necessary in the final cycles. Only 11 correlation coefficients in each of the final refinements exceed ± 0.70 and only one exceeds +0.81 (L_H^{33} for rings 2 and 3; 0.089 and 0.093 for the 173 and 298 K data). According to Hamilton's criterion the three-ring model R3ZHO is the best of all the structural models investigated (99% confidence level).

In general, the L^{33} values for the outer rings of the three-ring models increase with temperature (see *e.g.* Tables 2 and 8), although the values for the central rings do not. The L^{33} values, however, are very sensitive to the values of the distortion and occupancy factors, to the correction for the excess H-atom internal motion and to any constraints applied to the TLS parameters. The uncertainties associated with the L^{33} values for the outer rings are large. Detailed interpretations of the L^{33} values are probably not meaningful.

The distribution patterns at 173 and 298 K of model R3ZHO are similar (see Fig. 6). All C atoms of the central ring (ring 2) are located at or very near the centers of the density peaks (see Fig. 7) and the H atoms are at or very near the centers of the troughs. The final difference maps for R3ZHO (see Fig. 8) have less relief than the maps for any other model.

4. Discussion

This study shows that the phase transition at 164 K is not a simple order–disorder transition. The two-ring model, which would be expected to describe the disorder if the

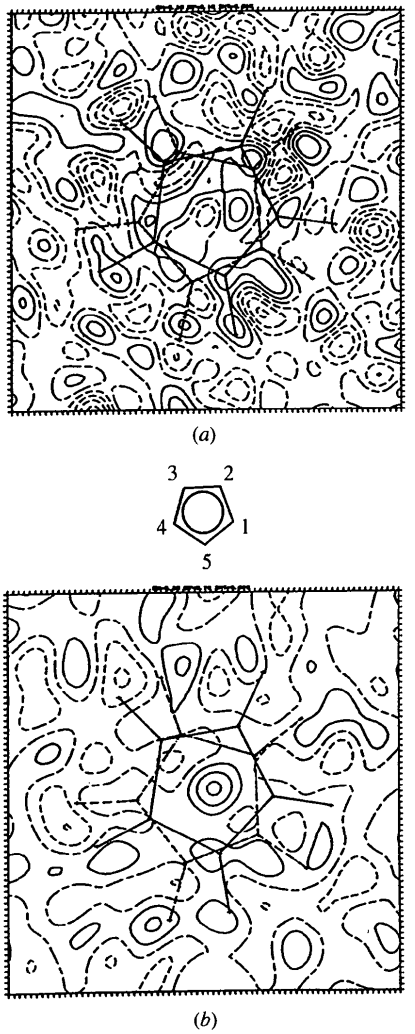

Fig. 5. Final difference maps through the best plane of the two Cp rings calculated after refinement with the model R2ZHO at (*a*) 173 and (*b*) 298 K. Contours are at intervals of 0.016 mm Å^{-3} in (*a*) and 0.010 mm Å^{-3} in (*b*). Solid, broken and dashed lines denote positive, zero and negative contours. The position of ring 1 is shown by a solid line and of ring 2 by a dashed line.

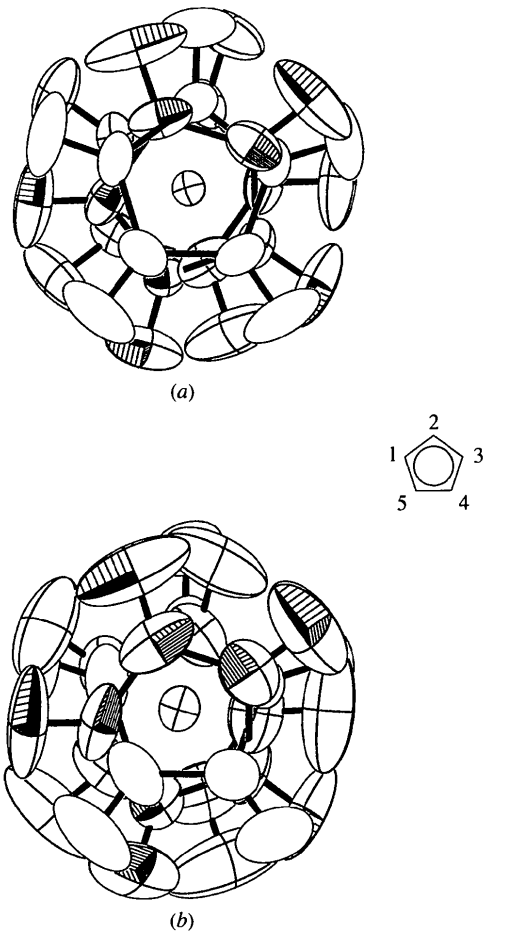

Fig. 6. Ellipsoid plot of the asymmetric unit after refinement with mode R3ZHO at (*a*) 173 and (*b*) 298 K. Boundary ellipses only are drawn for the atoms of ring 1. Principal and boundary ellipses are drawn fo the atoms of rings 2 and 3; shading has been added to the ellipsoid of ring 3.

phase transition corresponded to the loss of long-range order, is less satisfactory than more complex models. The potential-energy wells in the two phases must differ in important ways. The success of the three-ring model indicates that the potential-energy surface for in-plane ring rotation in the high-temperature phase is not simple.

This study confirms several of the suggestions about the disorder made previously. Willis (1961) found (see Takusagawa & Koetzle, 1979) that a model with 1/3 of the rings rotated by 36° [*i.e.* (1/2)(360/5)] around the approximate C_5 axis was more satisfactory than an ordered model. The R2ZHO model confirms that general conclusion (see Tables 1 and 5), although the angular separations between the two rings are less than 36° [22 (2)° at 173 K and 28 (2)° at 298 K; see Fig. 5]. Takusagawa & Koetzle (1979) suggested an angular displacement of ~24°. (NB Comparisons of these estimates are complicated by the separation of the ring centers.) Our results are also consistent with those of Calvarin, Berar & Clec'h (1982).

Takusagawa & Koetzle (1979) concluded that their model *B*, which incorporated third- and fourth-order tensors to account for curvilinear motion, anharmonic motion and/or disorder, was the most successful (see Table 1), even though the ratio of observations to variables was very low. Model R3ZHO achieves a comparable fit with many fewer parameters. The conclusions from the two studies are, however, the same: the potential-energy surface for rotation of the rings about the approximate C_5 axis is not simple.

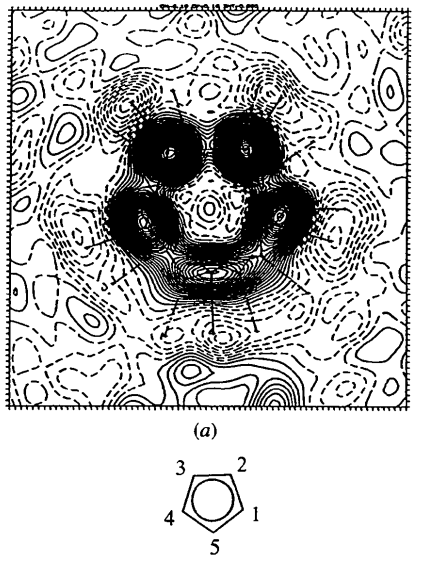

Fig. 7. Fourier maps through the best plane of the three Cp rings calculated after refinement with model R3ZHO at (*a*) 173 and (*b*) 298 K. Contours are at intervals of 0.08 mm Å^{-3} in (*a*) and 0.05 mm Å^{-3} in (*b*). Solid, broken and dashed lines denote positive, zero and negative contours, respectively. Rings 1, 2 and 3 are represented by solid, dashed and broken lines.

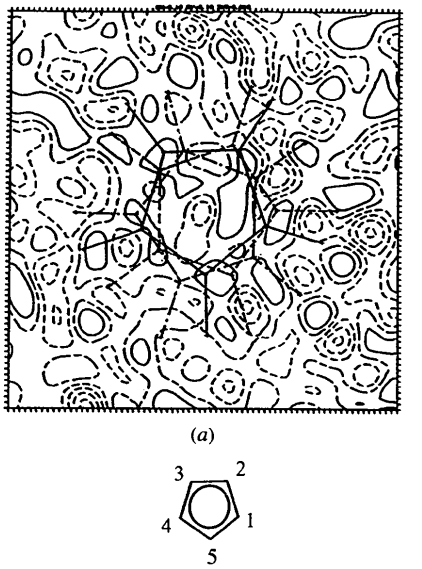

Fig. 8. Final difference-Fourier maps through the best plane of the three Cp rings calculated after refinement with model R3ZHO at (*a*) 173 and (*b*) 298 K. Contours are at intervals of 0.016 mm Å^{-3} in (*a*) and 0.010 mm Å^{-3} in (*b*). Solid, broken and dashed lines denote positive, zero and negative contours. Rings 1, 2 and 3 are represented by solid, dashed, and broken lines.

Table 8. *Thermal motion description for the model R3ZHO*

	At 173 K			At 298 K		
$\mathbf{U}_{Fe}$ (Å^2)	0.0301(8)	−0.0049 (5)	−0.0016 (6)	0.0412 (12)	−0.0064 (10)	−0.0008 (11)
		0.0216 (7)	0.0175 (6)		0.0365 (9)	0.0259 (11)
			0.0327 (8)			0.0547 (14)
T (Å^2)	0.040 (5)	−0.004 (2)	0.003 (2)	0.068 (7)	0.004 (4)	0.003 (4)
	0.034 (2)	−0.004 (1)	−0.002 (1)	0.045 (4)	−0.009 (3)	0.000 (3)
	0.043 (4)	0.005 (2)	0.000 (3)	0.080 (7)	−0.007 (3)	−0.011 (4)
		0.048 (3)	0.003 (2)		0.078 (5)	−0.003 (3)
		0.030 (3)	0.001 (2)		0.065 (6)	0.006 (3)
		0.036 (4)	−0.002 (3)		0.038 (5)	−0.003 (3)
			0.018 (3)			0.026 (5)
			0.014 (3)			0.027 (5)
			0.032 (5)			0.036 (6)
L (deg^2)	14.0 (5)	6.0 (3)	26.0 (7)	30.0 (9)	−13.0 (5)	−27.0 (12)
	22.0 (4)	−1.0 (2)	13.0 (6)	47.0 (10)	12.0 (6)	23.0 (8)
	17.0 (8)	9.0 (4)	−10.0 (10)	8.0 (8)	−9.0 (6)	5.0 (11)
		15.0 (5)	17.0 (7)		40.0 (9)	−6.0 (13)
		16.0 (4)	−2.0 (5)		18.0 (7)	−21.0 (8)
		15.0 (8)	−5.0 (10)		58.0 (12)	−66.0 (15)
			53.0 (14)			124.0 (25)
			60.0 (9)			53.0 (14)
			59.0 (17)			121.0 (27)
L_H^{33} (deg^2)			88.0 (12)			171.0 (24)
			78.0 (8)			67.0 (11)
			104.0 (15)			137.0 (21)
S (Å deg)	−0.17 (10)	0.46 (9)	0.16 (6)	0.34 (16)	1.01 (14)	0.20 (8)
	−0.03 (5)	0.06 (8)	0.06 (4)	−0.04 (14)	0.15 (17)	−0.07 (11)
	0.17 (11)	0.38 (11)	−0.11 (8)	0.53 (16)	0.34 (12)	0.01 (10)
	−0.56 (10)	0.18 (8)	−0.07 (6)	−0.49 (15)	−0.24 (15)	−0.05 (10)
	−0.21 (5)	0.10 (7)	0.06 (4)	−0.46 (13)	0.56 (14)	−0.07 (8)
	−0.38 (12)	0.01 (11)	−0.18 (8)	−0.93 (21)	0.29 (16)	0.08 (13)
	0.68 (16)	0.25 (17)	−0.01†	−1.13 (32)	0.10 (30)	−0.10†
	−0.10 (12)	−0.25 (10)	−0.07†	0.15 (17)	−0.76 (18)	−0.52†
	0.36 (15)	0.59 (17)	−0.17†	0.78 (32)	0.34 (26)	−0.82†

† Determined by the constraint tr(**S**) = 0.

The agreement factors for the 298 K data are always better for the 173 K data. Even though the 173 K data were measured at a temperature about 9 K above T_c, structural changes associated with the high-to-low-temperature transition may have already begun.

Monoclinic ferrocene can be compared with the isostructural vandocene, which undergoes no phase change upon cooling and which has normal ADP's at 108 K (Antipin & Boese, 1996). At higher temperatures refinement of a two-site disorder model (Antipin & Boese, 1996) gave a ring-plane rotation between the two sites of *ca* 36° and temperature-dependent occupancy factors (0.17/0.83 at 297 K and 0.35/0.65 at 357 K). Cobaltocene (Antipin, Boese, Augart & Schmidt, 1993) and nickelocene (Seiler & Dunitz, 1980) are isostructural with Cp_2V, but have residual disorder at 100 K. Antipin & Boese (1996) observed that increased ordering in Cp_2M, M = Co, Ni and V, is correlated with the metal–carbon distance, which is smallest in ferrocene (2.06 Å) and largest in vanadocene (2.27 Å). This study indicates that the potential-energy surface governing ring motion in monoclinic ferrocene is qualitatively different from the double-well potential found for the isostructural Cp_2M, M = Co, Ni and V series (Antipin & Boese, 1996).

Acknowledgement is made to the donors of the Petroleum Research Fund, administered by the American Chemical Society, for partial support of this research. Y. Fu thanks the Graduate School of the University of Kentucky for an Academic Year Fellowship. We also thank T. F. Koetzle for helpful discussions.

References

Antipin, M. Yu. & Boese, R. (1996). *Acta Cryst.* B**52**, 314–322.
Antipin, M. Yu., Boese, R., Augart, N. & Schmidt, G. (1993). *Struct. Chem.* **4**, 91–101.
Braga, D. (1992). *Chem. Rev.* **92**, 633–665.
Brock, C. P., Blackburn, J. R. & Haller, K. L. (1984). *Acta Cryst.* B**40**, 493–498.
Busing, W. R., Martin, K. O. & Levy, H. A. (1962). *ORFLS.* Report ORNL-TM-305. Oak Ridge National Laboratory, Tennessee, USA.
Calvarin, G. & Berar, J. F. (1975). *J. Appl. Cryst.* **8**, 380–385.
Calvarin, G., Berar, J. F. & Clec'h, G. (1982). *J. Phys. Chem. Solids*, **43**, 791–796.
Calvarin, G., Clec'h, G., Berar, J. F. & André, D. (1982). *J. Phys. Chem. Solids*, **43**, 785–790.
Clec'h, G., Calvarin, G., Berar, J. F. & Kahn, R. (1978). *C. R. Acad. Sci. Ser. C*, **286**, 315–317.

Cruickshank, D. W. J. (1956). *Acta Cryst.* **9**, 754–756.
Dunitz, J. D. (1993). In *Organic Chemistry: Its Language and Its State of the Art*, edited by M. V. Kisakuerek, pp. 9–23. Basel: Verlag Helvetica Chimica Acta.
Dunitz, J. D. (1995). *Acta Cryst.* B**51**, 619–631.
Dunitz, J. D. & Orgel, L. E. (1953). *Nature (London)*, **171**, 121–122.
Dunitz, J. D., Orgel, L. E. & Rich, A. (1956). *Acta Cryst.* **9**, 373–375.
Edwards, J. W. & Kington, G. L. (1962). *Trans. Faraday Soc.* **58**, 1323–1333.
Edwards, J. W., Kington, G. L. & Mason, R. (1960). *Trans. Faraday Soc.* **56**, 660–667.
Eiland, P. F. & Pepinsky, R. (1952). *J. Am. Chem. Soc.* **74**, 4971.
Fischer, E. O. & Pfab, W. (1952). *Z. Naturforsch. Teil B*, pp. 377—379.
Fu, Y. (1991). Ph.D. Thesis. University of Kentucky.
Hamilton, W. C. (1965). *Acta Cryst.* **18**, 502–510.
Johnson, C. N. (1970). *Thermal Neutron Diffraction*, edited by B. T. M. Willis, ch. 9. Oxford University Press.
Koester, L. & Yelon, W. B. (1983). Distributed by the IUCr Neutron Diffraction Commission.
Maverick, E. & Dunitz, J. D. (1987). *Molec. Phys.* **62**, 451–459.
Pawley, G. S. (1970). *Acta Cryst.* A**26**, 691–692.
Schomaker, V. & Trueblood, K. M. (1968). *Acta Cryst.* B**24**, 63–76.
Seiler, P. & Dunitz, J. D. (1979*a*). *Acta Cryst.* B**35**, 1068–1074.
Seiler, P. & Dunitz, J. D. (1979*b*). *Acta Cryst.* B**35**, 2020–2032.
Seiler, P. & Dunitz, J. D. (1980). *Acta Cryst.* B**36**, 2255–2260.
Shmueli, U. & Goldberg, I. (1974). *Acta Cryst.* B**30**, 573–578.
Strouse, C. E. (1970). *Acta Cryst.* A**26**, 604–608.
Takusagawa, F. & Koetzle, T. F. (1979). *Acta Cryst.* B**35**, 1074–1081.
Trueblood, K. N. (1978). *Acta Cryst.* A**34**, 950–954.
Willis, B. T. M. (1960). *Acta Cryst.* **13**, 1088.
Willis, B. T. M. (1961). AERE Report R3708. Harwell, Oxfordshire, England.